

Small-angle AVO response of PS-waves in tilted TI media

Jyoti Behura and Ilya Tsvankin

Center for Wave Phenomena, Colorado School of Mines, Golden, CO 80401

ABSTRACT

Field records for small source-receiver offsets often contain intensive converted PS-waves that cannot be generated in laterally homogeneous isotropic models. Among the most likely physical reasons for this converted energy is the presence of anisotropy on either side of the reflector. Here, we study the small-angle reflection coefficients of the split converted PS₁- and PS₂-waves (R_{PS_1} and R_{PS_2}) for a horizontal interface separating two transversely isotropic media with arbitrary orientations of the symmetry axis.

The normal-incidence reflection coefficients $R_{PS_1}(0)$ and $R_{PS_2}(0)$ vanish when both halfspaces have a horizontal symmetry plane, which happens if the symmetry axis is vertical or horizontal (i.e., if the medium is VTI or HTI). For a tilted symmetry axis in either medium, however, the magnitude of the reflection coefficients can reach substantial values close to 0.1, even if the strength of anisotropy is moderate. To study the influence of the orientation of the symmetry axis and the anisotropy parameters, we develop concise weak-contrast, weak-anisotropy approximations for the reflection coefficients and compare them with exact numerical results.

In particular, the analytic solutions show that the contributions of the Thomsen parameters ϵ and δ to the coefficients $R_{PS_1}(0)$ and $R_{PS_2}(0)$ are governed by simple functions of the symmetry-axis tilt ν , which have the same form for both halfspaces. If the symmetry-axis orientation and anisotropy parameters do not change across the interface, the normal-incidence reflection coefficients are insignificant, regardless of the strength of the velocity and density contrast. The AVO (amplitude variation with offset) gradients of the PS-waves are mostly influenced by the anisotropy of the incidence medium that causes shear-wave splitting and determines the partitioning of energy between the PS₁ and PS₂ modes.

Because of their substantial amplitude, small-angle PS reflections in TI media contain valuable information for anisotropic AVO inversion of multicomponent data. Our analytic solutions provide a foundation for linear AVO-inversion algorithms and can be used to guide nonlinear inversion based on the exact reflection coefficients.

Key words: converted wave, transverse isotropy, TTI media, reflection coefficient, AVO intercept, AVO gradient, azimuthal AVO

Introduction

In a number of case studies, significant converted wave energy was observed at zero and near-zero offsets (e.g., Thomsen, 2002). This phenomenon can be explained by several factors, including heterogeneity and the pres-

ence of nongeometrical waves (Tsvankin, 1995). However, neither heterogeneity nor nongeometrical waves can account for normal-incidence PS-wave reflections for layer-cake subsurface models and large distances between the source and the interface.

Here, we study the influence of anisotropy on the amplitude of PS-waves at small source-receiver offsets. We restrict ourselves to the TTI (transverse isotropy with a tilted symmetry axis) model and analyze the influence of the orientation of the symmetry axis and the anisotropy parameters on the PS-wave reflection coefficients. The main focus of the paper is on the normal-incidence PS-wave reflection coefficient that vanishes only when the reflector coincides with a symmetry plane in both halfspaces. If the reflector is horizontal, generation of converted energy at vertical incidence requires the symmetry axis in at least one of the halfspaces to deviate from both the vertical and horizontal directions.

We employ exact computation of the reflection coefficients as well as linearized solutions that help to understand the influence of various model parameters on the PS-wave reflectivity. Approximate reflection and transmission coefficients for isotropic media can be found in Aki and Richards (2002) and Shuey (1985). Banik (1987), Thomsen (1993) and Rüger (1996, 1997, 1998) derived approximate P-wave reflection coefficients for VTI (TI with a vertical symmetry axis) and HTI (TI with a horizontal symmetry axis) media. Rüger's results can be also applied in the symmetry planes of orthorhombic media. Pšenčík and Vavryčuk (1998) and Vavryčuk and Pšenčík (1998) obtained weak-contrast, weak-anisotropy P-wave reflection and transmission coefficients for arbitrarily anisotropic media.

Closed-form solutions for the reflection coefficients of PS-waves in isotropic media can be found in Donati (1998), Larsen *et al.* (1999), Alvarez *et al.* (1999) and Nefedkina and Buzlukov (1999). Rüger (1996) developed approximate expressions for the PS-wave reflection coefficients in VTI media and the symmetry planes of HTI media. However, as mentioned above, the normal-incidence reflection coefficients of mode conversions go to zero in both VTI and HTI media. Weak-contrast, weak-anisotropy approximations for PS-wave reflection and transmission coefficients in arbitrarily anisotropic media were presented by Vavryčuk (1999), Jílek (2000) and Artola *et al.* (2003). Jílek (2001) also developed algorithms for the joint inversion of PP- and PS-wave reflection coefficients in azimuthally anisotropic media.

Jílek (2000) and Vavryčuk (1999) pointed out that the normal-incidence PS-wave reflection coefficients do not vanish for nonzero stiffnesses c_{34} and/or c_{35} on either side of the reflector. Artola *et al.* (2003) demonstrated the presence of normal-incidence PS-wave energy in synthetic seismograms computed for azimuthally anisotropic models. Here, we show that the tilt of the symmetry axis in TI media can create relatively strong zero-offset PS reflections from horizontal interfaces. Application of the weak-contrast, weak-anisotropy approximations helps to identify the parameter combinations responsible for both zero-offset reflection coefficients and AVO gradients of PS-waves.

1 ANALYTIC BACKGROUND

We start by setting up the system of linear equations that can be used to compute the exact reflection/transmission coefficients from the boundary conditions. The approximate (linearized) reflection/transmission coefficients are then obtained by applying the first-order perturbation theory.

1.1 Exact solution of the reflection/transmission problem

The reflection/transmission problem for a given incident wave is solved by satisfying the boundary conditions at the reflector. For a welded contact of the two halfspaces, these boundary conditions are the continuity of traction and displacement, which can be written in the following compact form:

$$\mathbf{C} \cdot \mathbf{U} = \mathbf{B}, \quad (1)$$

where \mathbf{C} corresponds to the displacement-stress matrix for the reflected and transmitted waves, \mathbf{B} is the displacement-stress vector of the incident wave, and \mathbf{U} is the vector of the reflection and transmission coefficients of the waves P, S_1 and S_2 :

$$\mathbf{C} = \begin{bmatrix} g_1^{(1)} & g_1^{(2)} & g_1^{(3)} & -g_1^{(4)} & -g_1^{(5)} & -g_1^{(6)} \\ g_2^{(1)} & g_2^{(2)} & g_2^{(3)} & -g_2^{(4)} & -g_2^{(5)} & -g_2^{(6)} \\ g_3^{(1)} & g_3^{(2)} & g_3^{(3)} & -g_3^{(4)} & -g_3^{(5)} & -g_3^{(6)} \\ X_1^{(1)} & X_1^{(2)} & X_1^{(3)} & -X_1^{(4)} & -X_1^{(5)} & -X_1^{(6)} \\ X_2^{(1)} & X_2^{(2)} & X_2^{(3)} & -X_2^{(4)} & -X_2^{(5)} & -X_2^{(6)} \\ X_3^{(1)} & X_3^{(2)} & X_3^{(3)} & -X_3^{(4)} & -X_3^{(5)} & -X_3^{(6)} \end{bmatrix}, \quad (2)$$

$$\mathbf{B} = - \left[g_1^{(0)}, g_2^{(0)}, g_3^{(0)}, X_1^{(0)}, X_2^{(0)}, X_3^{(0)} \right]^T, \quad (3)$$

$$\mathbf{U} = \left[R_{S1}, R_{S2}, R_P, T_{S1}, T_{S2}, T_P \right]^T. \quad (4)$$

Here the superscript denotes the reflected/transmitted modes according to the following convention:

0–incident wave; 1–reflected S_1 -wave; 2–reflected S_2 -wave; 3–reflected P-wave; 4–transmitted S_1 -wave; 5–transmitted S_2 -wave; 6–transmitted P-wave. In equation (2), $g(N)$ and $X(N)$ are the polarization and amplitude-normalized traction vectors, respectively, obtained by solving the Christoffel equation. Equation (1) can be solved numerically for \mathbf{U} to compute the reflection/transmission coefficients.

1.2 Weak-contrast, weak-anisotropy approximation

The main goal of using linearized approximations here is to gain physical insight into the dependence of the reflection coefficients on the medium parameters and incidence angle. Following the approach of Vavryčuk and Pšenčík (1998) and Jílek (2000), we linearize the boundary conditions by assuming a weak contrast in the elastic parameters across the interface and weak anisotropy

in both halfspaces (see Appendix A). A homogeneous isotropic full space divided by a fictitious planar interface is taken as the background medium. The elastic parameters $a_{ijkl} = c_{ijkl}/\rho$ (density-normalized stiffness coefficients) are expressed as small perturbations δa_{ijkl} from the background values. The exact boundary conditions [equation (1)] are then linearized in terms of the small perturbations to find approximate PS-wave reflection coefficients.

Consider an incident P-wave traveling in the negative z -direction in the $[x, z]$ -plane; the reflector coincides with the plane $z = 0$. The slowness vectors of the incident, reflected, and transmitted waves in the background medium can be written as follows (Figure 1):

$$\begin{aligned} \mathbf{p}^{0(0)} &= \mathbf{p}^{0(6)} = [p_1^0, 0, -p_3^{0P}], \\ \mathbf{p}^{0(1)} &= \mathbf{p}^{0(2)} = [p_1^0, 0, p_3^{0S}], \\ \mathbf{p}^{0(3)} &= [p_1^0, 0, p_3^{0P}], \\ \mathbf{p}^{0(4)} &= \mathbf{p}^{0(5)} = [p_1^0, 0, -p_3^{0S}]. \end{aligned} \quad (5)$$

The P-wave unit polarization vectors in the isotropic background are given by

$$\begin{aligned} \mathbf{g}^{0(0)} &= \mathbf{g}^{0(6)} = \alpha \mathbf{p}^{0(0)}, \\ \mathbf{g}^{0(3)} &= \alpha \mathbf{p}^{0(3)}, \end{aligned} \quad (6)$$

where α is the P-wave velocity in the background.

1.3 Polarization angle

The SV- and SH-components are obtained by projecting the S-wave polarization vector in the background onto the incidence $[x, z]$ plane and the direction orthogonal to it, respectively. In anisotropic media, however, for the perturbation approach to work, the chosen polarization vectors in the background isotropic medium ($\mathbf{g}^{0(1)}$ and $\mathbf{g}^{0(2)}$) should be close to the actual polarizations ($\mathbf{g}^{(1)}$ and $\mathbf{g}^{(2)}$) (Jech and Pšenčík, 1989). So the SV and SH-wave polarizations (\mathbf{g}^{SV} and \mathbf{g}^{SH}) in the background isotropic medium have to be rotated by an angle Φ called the ‘‘polarization angle,’’ which is defined uniquely (except for singular directions), as shown by Jech and Pšenčík (1989). Since the polarization angle is neither a linear function of the perturbations δa_{ijkl} nor is it necessarily small, the presence of Φ complicates the computation of the analytic expressions for the PS-wave reflection coefficients.

If the polarization angle is known, the polarization vectors of the S_1^0 and S_2^0 -waves ($\mathbf{g}^{0(1)}$ and $\mathbf{g}^{0(2)}$) can be determined by rotating the SV- and SH-wave polarization vectors counter-clockwise by the angle Φ in the plane perpendicular to the background slowness vector $\mathbf{p}^{0(1)}$ (Figure 1). Thus, $\mathbf{g}^{0(1)}$ and $\mathbf{g}^{0(2)}$ are given by

$$\begin{aligned} \mathbf{g}^{0(1)} &= [\beta p_3^{0S} \cos \Phi, \sin \Phi, -\beta p_1^0 \cos \Phi], \\ \mathbf{g}^{0(2)} &= [-\beta p_3^{0S} \sin \Phi, \cos \Phi, \beta p_1^0 \sin \Phi], \end{aligned} \quad (7)$$

where β is the S-wave velocity in the background. Equa-

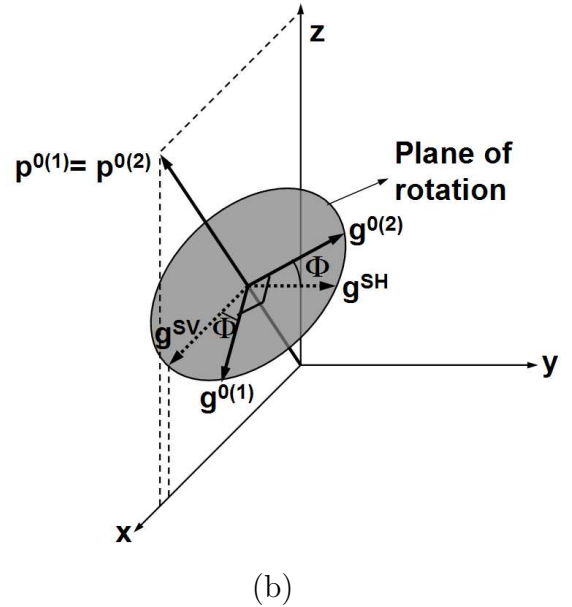
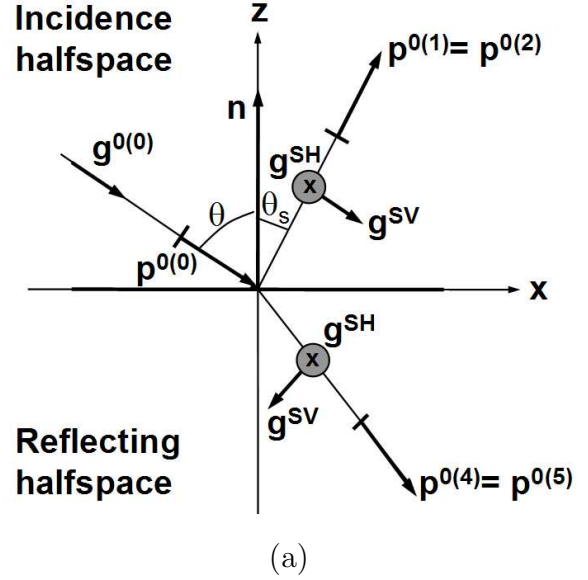


Figure 1. (a) Conventions used in solving the reflection/transmission problem. The incidence $[x, z]$ -plane contains the interface normal \mathbf{n} and the background P-wave slowness vector $\mathbf{p}^{0(0)}$. The background S-wave slowness vectors are denoted by $\mathbf{p}^{0(1)} = \mathbf{p}^{0(2)}$ (reflected) and $\mathbf{p}^{0(4)} = \mathbf{p}^{0(5)}$ (transmitted); θ and θ_s are the phase angles of the incident P-wave and reflected S-wave. The polarization vector of the incident P-wave in the background medium is $\mathbf{g}^{0(0)}$, while the SV- and SH-wave polarizations vectors are \mathbf{g}^{SV} and \mathbf{g}^{SH} , respectively. (b) $\mathbf{g}^{0(1)}$ and $\mathbf{g}^{0(2)}$ are the chosen polarization vectors of the reflected S_1 - and S_2 -waves, respectively, in the background medium. These vectors are obtained by rotating \mathbf{g}^{SV} and \mathbf{g}^{SH} by the angle Φ (polarization angle) in the plane orthogonal to the slowness vector $\mathbf{p}^{0(1)}$. If the incidence halfspace is isotropic or VTI, $\Phi = 0$ [after Jilek (2000)].

tion (7) shows that when the medium is isotropic and $\Phi = 0$ (Jech and Pšenčík, 1989), S_1^0 reduces to SV and S_2^0 reduces to SH. Similarly, the polarization vectors of the transmitted S-waves can be written as

$$\begin{aligned} \mathbf{g}^{0(4)} &= [-\beta p_3^{0S} \cos \Psi, \quad \sin \Psi, \quad -\beta p_1^0 \cos \Psi], \\ \mathbf{g}^{0(5)} &= [\beta p_3^{0S} \sin \Psi, \quad \cos \Psi, \quad \beta p_1^0 \sin \Psi], \end{aligned} \quad (8)$$

where Ψ is the corresponding polarization angle. Since we are concerned with the reflected S-waves only, computation of Ψ is unnecessary because $\mathbf{g}^{0(4)}$ and $\mathbf{g}^{0(5)}$ are not involved in the linearized reflection coefficients [equation (A11)].

When the incidence halfspace is anisotropic, Φ is generally nonzero. If the medium is TTI, the polarization vector of the PS_1 -wave lies in the plane formed by the symmetry axis and the PS_1 slowness vector (i.e., it is the PSV-wave in the coordinate system in which the symmetry axis is taken as vertical) while the PS_2 -wave would be polarized orthogonal to that plane. (Note that PS_1 is not necessarily the fast PS mode.) Thus, in this case Φ is the angle between the background SV-wave polarization vector and the plane formed by $\mathbf{p}^{0(1)}$ and the symmetry axis of the incident TTI halfspace. Using simple vector algebra and dropping the cubic and higher-order terms in $\sin \theta$, we find

$$\cos \Phi \approx \frac{1}{2g^2 A} (2g^2 \cos \phi_1 \sin \nu_1 + 2g \cos \nu_1 \sin \theta + \cos \phi_1 \sin \nu_1 \sin^2 \theta), \quad (9)$$

where

$$A \equiv \left(\sin^2 \nu_1 + \frac{\cos \phi_1 \sin 2\nu_1 \sin \theta}{g} + \frac{(\cos^2 \nu_1 - \sin^2 \nu_1 \cos^2 \phi_1) \sin^2 \theta}{g^2} \right)^{1/2}.$$

Here ν_1 and ϕ_1 are the tilt (i.e., the angle with the vertical) and azimuth, respectively, of the symmetry axis of the incidence TI halfspace, and $g \equiv \alpha/\beta$. Although Φ can be computed from equation (9), its presence complicates the approximate PS-wave reflection coefficients. Although Φ is independent of the anisotropic parameters (except for the tilt of the symmetry axis), it depends on the incidence angle in a rather complicated way. For an incident TTI halfspace, $\Phi \neq 0$ whenever the incidence plane is different from the vertical symmetry-axis plane (i.e., from the vertical plane that contains the symmetry axis) of the incidence halfspace.

In general, Φ cannot be linearized in θ without assuming that $\sin^2 \nu_1$ is sufficiently large, except for the special case of normal incidence ($\theta = 0$) when Φ reduces to ϕ_1 [equation(9)]. This complication prevents us from deriving fully linearized oblique-incidence reflection coefficients for TI media with arbitrary orientation of symmetry axis. For an incident VTI halfspace ($\nu_1 = 0^\circ$) $\Phi = 0$, and for an incident HTI halfspace ($\nu_1 = 90^\circ$), Φ can be linearized in terms of the medium

parameters [equation (9)]. The orientation of the symmetry axis of the reflecting TI halfspace does not pose any problems in the linearization of the reflection coefficients because it does not contribute to Φ . Because of the above constraints, linearized PS-wave reflection coefficients for oblique incidence angles are given here only if the incidence halfspace is isotropic, VTI, HTI, or TTI with the symmetry axis confined to the incidence plane. For oblique incidence of P-waves in all other models, we analyze only the exact reflection coefficients.

2 NORMAL-INCIDENCE REFLECTION COEFFICIENT

The normal-incidence reflection coefficient is also called the ‘‘intercept’’ in amplitude-variation-with-offset (AVO) analysis. The general linearized equation for small-angle PS-wave reflection coefficients can be written as (Thomsen, 2002),

$$R_{PS} = R_{PS}(0) + G \sin \theta, \quad (10)$$

where $R_{PS}(0)$ is the normal-incidence reflection coefficient and G is the AVO gradient. In this section, we discuss the normal-incidence reflection coefficient; the AVO gradient is analyzed next.

2.1 Isotropic/TTI interface

Consider the model that includes an incidence isotropic halfspace overlying a reflecting TTI halfspace. The normal-incidence PS-wave in this case is polarized in the symmetry-axis plane of the reflecting halfspace (Figure 2). In general, the reflected PS-wave can be represented as the vector sum of the PSV- and PSH-waves. For normal incidence, however, the incidence plane is undefined, and it is convenient to study the PS-wave as a whole.

The linearized PS-wave normal-incidence reflection coefficient is given by

$$R_{PS}(0) = \frac{g^2 \sin 2\nu_2 [\cos 2\nu_2 (\delta_2 - \epsilon_2) + \epsilon_2]}{4(1+g)} \quad (11)$$

$$= \frac{g^2}{4(1+g)} \frac{1}{V_{P,2}} \left. \frac{dV_{P,2}(\theta)}{d\theta} \right|_{\theta=0} \quad (12)$$

where $V_{P,2}$ is the P-wave phase velocity in the reflecting halfspace. It is interesting that the normal-incidence PS-wave reflection coefficient is proportional to the first derivative of the P-wave phase velocity computed at $\theta = 0$. Although this derivative is supposed to be linearized to make equation (12) equivalent to equation (11), the accuracy of the weak-contrast, weak-anisotropy approximation can be increased by using the exact value of this derivative in equation (12) (Figure 3).

The very existence of the normal-incidence PS reflection is caused by the tilt of the symmetry axis away

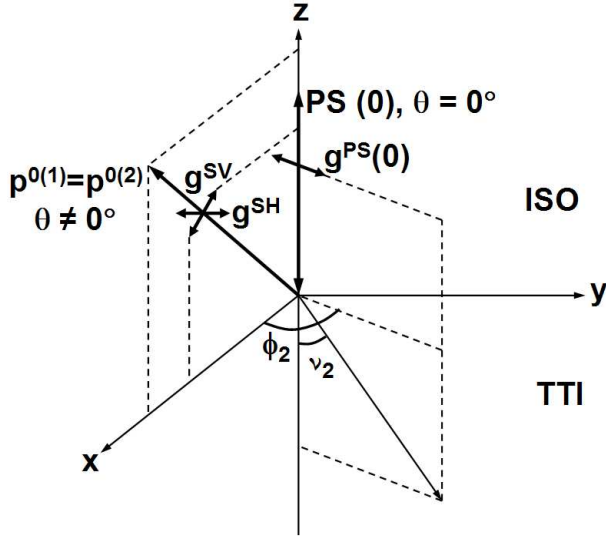


Figure 2. For an isotropic incidence halfspace overlying a TTI reflecting halfspace, the PS-wave at normal incidence is polarized (vector g^{PS}) in the symmetry-axis plane. For oblique incidence, we analyze the two components of the PS-wave (PSV and PSH) separately.

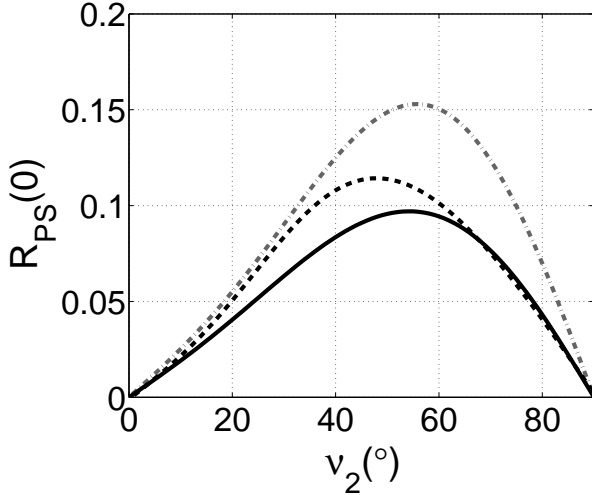


Figure 3. Accuracy of the weak-contrast, weak-anisotropy approximation for the normal-incidence PS-wave reflection coefficient. The solid black line is the exact coefficient for an isotropic/TTI interface, the dashed black line is computed using equation (12) with the exact first derivative of the P-wave phase velocity, and the dash-dotted gray line marks the fully linearized approximation (11). The parameters of the incidence isotropic halfspace are $V_{P,1} = 2.9$ km/s, $V_{S,1} = 1.5$ km/s, and $\rho_1 = 2$ gm/cm³. The parameters of the reflecting TTI halfspace are $V_{P0,2} = 3.3$ km/s, $V_{S0,2} = 1.8$ km/s, $\rho_2 = 2.2$ gm/cm³, $\epsilon_2 = 0.4$, $\delta_2 = 0.2$, $\gamma_2 = 0.11$, and $\phi_2 = 30^\circ$.

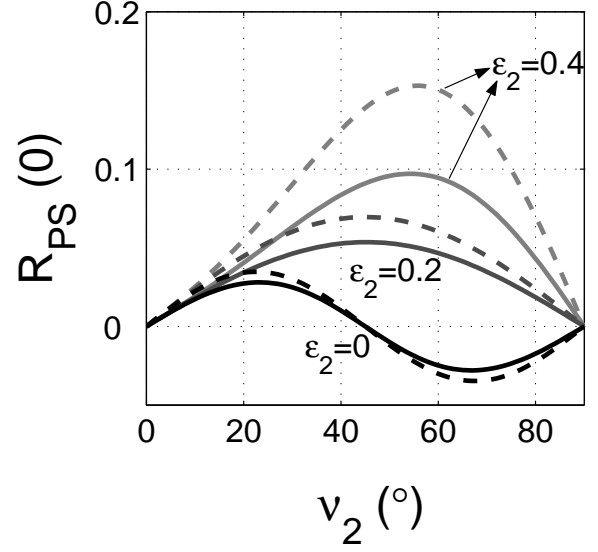


Figure 4. The normal-incidence PS-wave reflection coefficient for an isotropic/TTI interface as a function of tilt ν_2 of the symmetry axis and the parameter ϵ_2 . The solid lines mark the exact $R_{PS}(0)$, the dashed lines represent the linearized approximation (11). The parameters of the incidence isotropic halfspace are $V_{P,1} = 2.9$ km/s, $V_{S,1} = 1.5$ km/s, and $\rho_1 = 2$ gm/cm³. The parameters of the reflecting TTI halfspace are $V_{P0,2} = 3.3$ km/s, $V_{S0,2} = 1.8$ km/s, $\rho_2 = 2.2$ gm/cm³, $\delta_2 = 0.2$, $\gamma_2 = 0.11$, and $\phi_2 = 30^\circ$.

from the vertical and horizontal directions. Therefore, $R_{PS}(0)$ goes to zero for both VTI ($\nu_2 = 0^\circ$) and HTI ($\nu_2 = 90^\circ$) media; the dependence on ν_2 may have minima and maxima at intermediate tilts. For the model in Figure 4, $R_{PS}(0)$ attains values as high as 0.1 for $\epsilon_2 = 0.4$; in general, the magnitude of $R_{PS}(0)$ increases with ϵ_2 . Apart from the anisotropy parameters, the normal-incidence reflection coefficient also increases with $g \equiv \alpha/\beta$.

The linearized $R_{PS}(0)$ is close to the exact value for models approaching VTI and HTI, but the approximation deteriorates for higher absolute values of $R_{PS}(0)$ (Figures 3 and 4). The accuracy of the linearized expressions also decreases with g , and the approximation may break down for soft rocks with high V_P/V_S ratios.

The dependence of $R_{PS}(0)$ on the parameters ϵ_2 , δ_2 and ν_2 in Figures 4 and 5 can be explained using approximation (11). The influence of ϵ_2 and δ_2 on $R_{PS}(0)$ strongly depends on the tilt ν_2 of the symmetry axis (Figure 6). If the function of ν_2 multiplied with ϵ_2 and δ_2 becomes zero, the corresponding anisotropy parameter makes no contribution to $R_{PS}(0)$. For example, according to approximation (11), δ_2 should have no influence on the $R_{PS}(0)$ at $\nu_2 = 45^\circ$, which is confirmed by the exact $R_{PS}(0)$ in Figure 5. For small tilts ν_2 , δ_2 has a greater influence on $R_{PS}(0)$ than does ϵ_2 , while for larger ν_2 , ϵ_2 largely determines the value of $R_{PS}(0)$.

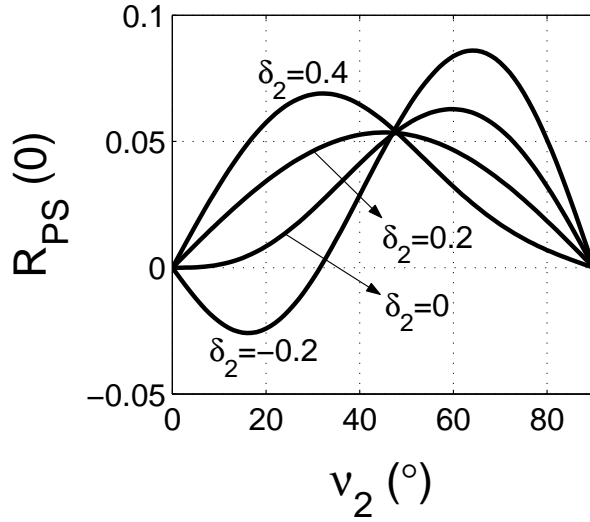


Figure 5. Exact coefficient $R_{PS}(0)$ for an isotropic/TTI interface as a function of the tilt ν_2 and the parameter δ_2 . Except for δ_2 and $\epsilon_2 = 0.2$, the model parameters are the same as in Figure 4.

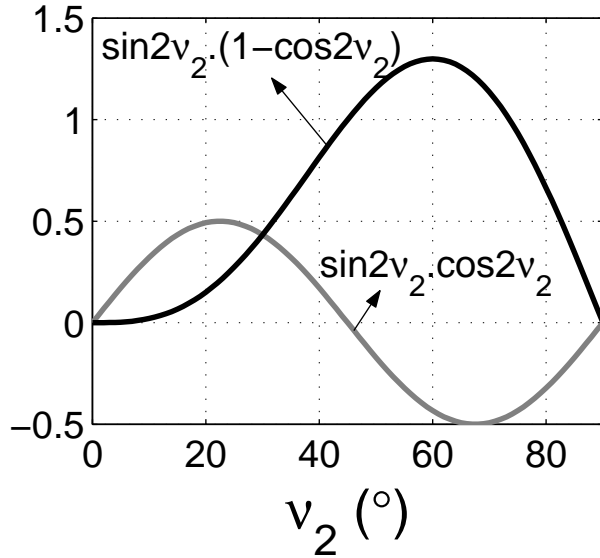


Figure 6. Functions of ν_2 multiplied with ϵ_2 (black line) and δ_2 (gray line) in equation (11). These curves help to explain the influence of ϵ_2 and δ_2 on $R_{PS}(0)$ for different tilts ν_2 in Figures 4 and 5.

This dependence of $R_{PS}(0)$ on ϵ and δ is explained by the behavior of the P-wave phase-velocity function in TI media. At small angles with the symmetry axis, P-wave velocity is controlled by δ , while the contribution of ϵ increases toward the isotropy plane (e.g., Tsvankin, 2001).

2.2 TTI/TTI interface

Next, we consider the normal-incidence PS reflection for a model in which the incidence halfspace is also TTI. In isotropic media, an incident P-wave excites a single converted (PSV) mode because the symmetry prohibits the generation of PSH conversions. When the incidence halfspace is anisotropic, the PS reflection splits into the PS_1 and PS_2 modes that have different normal-incidence reflection coefficients ($R_{PS_1}(0)$ and $R_{PS_2}(0)$) and AVO gradients. To understand the influence of the parameters of both halfspaces, we study the linearized approximations for $R_{PS_1}(0)$ and $R_{PS_2}(0)$.

2.2.1 Special case of aligned symmetry planes

If the azimuth of the symmetry axis is the same above and below the reflector ($\phi_1 = \phi_2$), the vertical plane that contains both symmetry axes represents a plane of symmetry for the whole model. In this case, the P-wave at normal incidence excites only one (PS_1) wave polarized in the symmetry-axis plane:

$$R_{PS_1}(0) = \frac{g^2}{4(1+g)} \left\{ -\sin 2\nu_1 [\cos 2\nu_1 (\delta_1 - \epsilon_1) + \epsilon_1] + \sin 2\nu_2 [\cos 2\nu_2 (\delta_2 - \epsilon_2) + \epsilon_2] \right\} \quad (13)$$

$$= \frac{g^2}{4(1+g)} \left(-\frac{1}{V_{P0,1}} \frac{dV_{P,1}(\theta)}{d\theta} \Big|_{\theta=0} + \frac{1}{V_{P0,2}} \frac{dV_{P,2}(\theta)}{d\theta} \Big|_{\theta=0} \right), \quad (14)$$

$$R_{PS_2}(0) = 0. \quad (15)$$

The coefficient $R_{PS_1}(0)$ is a function of both tilts (ν_1 and ν_2) and all anisotropy parameters except for γ_1 and γ_2 – the parameters responsible for SH-wave propagation in TI media.

$R_{PS_1}(0)$ vanishes when each of the halfspaces is either VTI or HTI, and the reflector represents a symmetry plane for the whole model. The term involving ν_1 , ϵ_1 , and δ_1 in equation (13) coincides by absolute value with that involving ν_2 , ϵ_2 , and δ_2 . So the conclusions drawn above for ν_2 , ϵ_2 , and δ_2 (Figure 6) apply to ν_1 , ϵ_1 , and δ_1 as well. If both TI halfspaces have the same orientation of the symmetry axes and the same parameters ϵ and δ , $R_{PS_1}(0)$ vanishes, even though there may be a jump in the other parameters across the interface. This result, however, is valid only in the weak-contrast, weak-anisotropy limit.

2.2.2 General TTI/TTI model

Suppose the symmetry axis has an arbitrary orientation in both halfspaces. Then a P-wave at normal-incidence excited both PS modes, and the approximate solutions

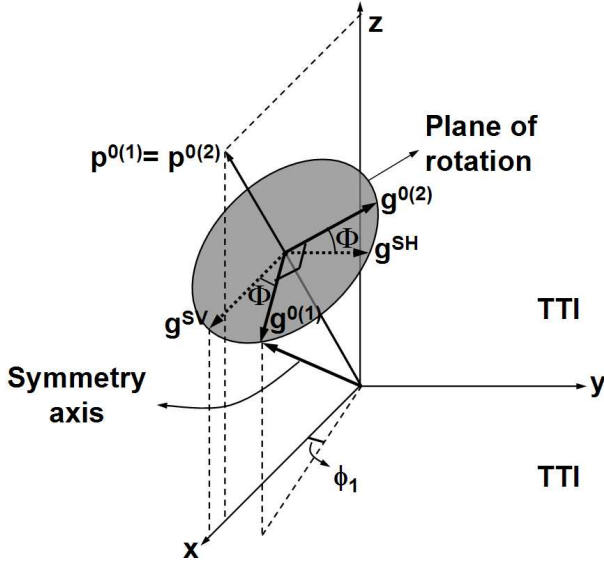


Figure 7. For an incidence TI halfspace, $\mathbf{g}^{0(1)}$ lies in the plane formed by the slowness vector and the symmetry axis (i.e., it would correspond to the SV-wave, if the symmetry axis were vertical), while $\mathbf{g}^{0(2)}$ is perpendicular to this plane (SH-wave).

for $R_{PS_1}(0)$ and $R_{PS_2}(0)$ are as follows:

$$R_{PS_1}(0) = \frac{g^2}{4(1+g)} \left\{ -\sin 2\nu_1 [\cos 2\nu_1 (\delta_1 - \epsilon_1) + \epsilon_1] + \cos(\phi_2 - \phi_1) \sin 2\nu_2 [\cos 2\nu_2 (\delta_2 - \epsilon_2) + \epsilon_2] \right\} \quad (16)$$

$$= \frac{g^2}{4(1+g)} \left(-\frac{1}{V_{P0,1}} \frac{dV_{P,1}(\theta)}{d\theta} \Big|_{\theta=0} + \cos(\phi_2 - \phi_1) \frac{1}{V_{P0,2}} \frac{dV_{P,2}(\theta)}{d\theta} \Big|_{\theta=0} \right), \quad (17)$$

$$R_{PS_2}(0) = \frac{g^2}{4(1+g)} \left\{ \sin(\phi_2 - \phi_1) \sin 2\nu_2 [\cos 2\nu_2 (\delta_2 - \epsilon_2) + \epsilon_2] \right\} \quad (18)$$

$$= \frac{g^2}{4(1+g)} \sin(\phi_2 - \phi_1) \frac{1}{V_{P0,2}} \frac{dV_{P,2}(\theta)}{d\theta} \Big|_{\theta=0}. \quad (19)$$

It is clear from the symmetry of the above model (TTI/TTI), that the normal-incidence reflection coefficients should depend just on the difference $\phi_2 - \phi_1$ which is confirmed by equations (16)–(19). Indeed, a simultaneous azimuthal rotation of both symmetry axes can only change the azimuthal direction of the polarization vectors of the PS-waves. When the vertical symmetry planes of the two TI halfspaces coincide ($\phi_1 = \phi_2$), equations (17) and (19) reduce to equations (14) and (15), respectively. Note that the terms involving the tilt of the symmetry axis and the anisotropy parameters in equations (16) and (18) have the same form as the cor-

responding terms for the simpler isotropic/TTI model examined above.

3 AVO GRADIENTS

The AVO gradients of the split PS-waves can be computed numerically by estimating the best-fit initial slope of the exact reflection coefficient expressed as a function of $\sin \theta$. In the linearized weak-anisotropy, weak-contrast approximation, the gradient G is obtained explicitly as the multiplier of $\sin \theta$ [equation (10)]. The linearized approximations for the PS-wave AVO gradients are given in Appendix B.

3.1 Isotropic/TTI interface

For the isotropic/TTI interface, only the gradient G_{PS_1} contains both isotropic and anisotropic terms, while G_{PS_2} is purely anisotropic [equations (B1) and (B2)]. The expression for G_{PS_1} reduces to the familiar gradient for isotropic media (e.g., Nefedkina and Buzlukov, 1999), if $\epsilon_2 = \delta_2 = \gamma_2 = 0$.

In the linearized approximation, the reflection coefficients for isotropic media coincide with the isotropic terms in the coefficients for the isotropic/TTI interface. Numerical testing shows that the AVO gradient is not significantly distorted by the anisotropy for common values of the vertical-velocity ratio g (Figure 8). The influence of the anisotropy in the reflecting halfspace changes primarily the normal-incidence coefficient $R_{PS}(0)$ that goes to zero in the isotropic model. Although the AVO gradients of both PS-waves vary with azimuth, their average values are close to those for isotropic media, and the magnitude of the azimuthal variations is relatively small.

Since the dependence of the AVO gradients on the parameters of the reflecting medium is rather complicated, in particular for the PS₁-wave [equation (B1)], we studied the behavior of the exact gradients using numerical modeling. As was the case for $R_{PS}(0)$, the influence of ϵ_2 on both G_{PS_1} and G_{PS_2} increases with the tilt ν_2 , while that of δ_2 becomes smaller. The contribution of γ_2 to both AVO gradients also increases with ν_2 .

The PS₂-wave vanishes for a reflecting VTI halfspace when the reflected PS-wave is polarized in the symmetry-axis plane of the incidence medium. Therefore, the gradient G_{PS_2} increases as the symmetry axis deviates from the vertical. G_{PS_2} also goes to zero when the symmetry axis is confined to the incidence plane or is perpendicular to it.

3.2 TTI/TTI interface

The AVO gradients of the PS₁- and PS₂-waves for a TTI/TTI interface [equations (B3) and (B4)] are de-

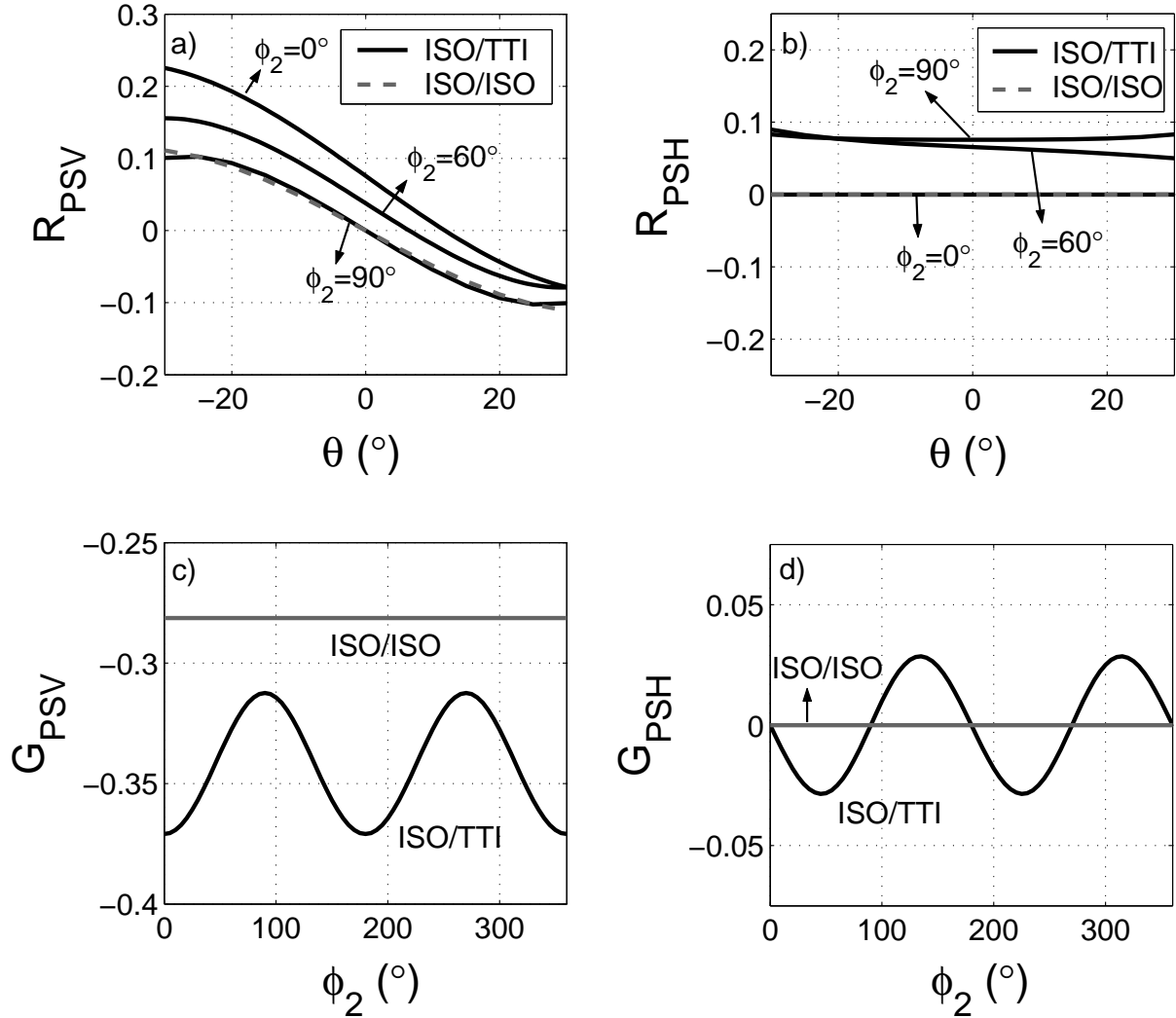


Figure 8. Exact PS-wave reflection coefficients (top row) and AVO gradients (bottom row) for isotropic/isotropic and isotropic/TTI interfaces. The velocity and density contrasts for both models are the same: $\Delta\rho = 0.2 \text{ gm/cm}^3$, $\bar{\rho} = 2.1 \text{ gm/cm}^3$, $\Delta\beta = 0.3 \text{ km/s}$, $\beta = 1.65 \text{ km/s}$, $\Delta\alpha = 0.4 \text{ km/s}$, $\alpha = 3.1 \text{ km/s}$, and $g = 1.88$. The anisotropy parameters of the reflecting TTI halfspace are $\epsilon_2 = 0.3$, $\delta_2 = 0.15$, $\gamma_2 = 0.11$, and $\nu_2 = 60^\circ$.

rived in Appendix B for the special case of the incidence plane containing the symmetry axis of the upper halfspace. We also present numerical results for an arbitrary orientation of the symmetry axis of the incidence medium.

In agreement with the linearized approximations (B3) and (B4), the anisotropy parameters ϵ_1 and δ_1 influence only G_{PS_1} while γ_1 influences only G_{PS_2} (Figures 9 and 10). To explain this result valid for an arbitrary orientation of the symmetry axis of the incidence halfspace, note that the PS_1 -wave would be the PSV mode if the symmetry axis were vertical, and the PS_2 -wave would be the PSH (transversely polarized) mode. The P- and SV-wave propagation in TI media

is governed only by ϵ and δ , while the SH-wave velocity is controlled by γ (Tsvankin, 2001).

As shown earlier, when the incidence medium is isotropic, the gradient G_{PS_1} contains both isotropic and anisotropic terms, while G_{PS_2} is purely anisotropic. If the incidence halfspace is TTI with the symmetry axis not confined to the incidence plane, then there are no purely isotropic terms in either gradient, as demonstrated for the special case of the HTI reflecting medium by equations (B5) and (B6). The influence of the anisotropy in the upper halfspace leads to a substantial deviation of the gradients computed for a TTI/TTI interface from those for the corresponding isotropic model (compare Figures 11 and 8).

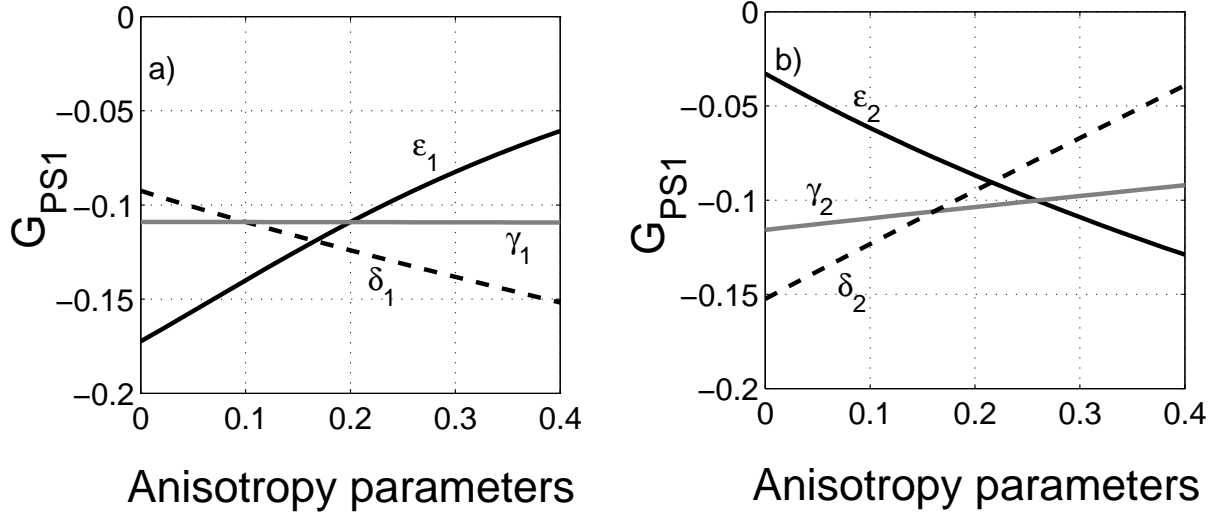


Figure 9. Exact AVO gradient of the PS_1 -wave for a TTI/TTI interface as a function of the anisotropy parameters in the (a) incidence and (b) reflecting halfspaces. The incidence plane makes the angle $\phi_1 = 60^\circ$ with the symmetry-axis plane of the incidence halfspace. The medium parameters of the incidence TTI halfspace are $V_{P0,1} = 2.9$ km/s, $V_{S0,1} = 1.5$ km/s, $\rho_1 = 2$ gm/cm³, $\epsilon_1 = 0.2$, $\delta_1 = 0.1$, $\gamma_1 = 0.1$, and $\nu_1 = 60^\circ$. The parameters of the reflecting halfspace are $V_{P0,2} = 3.3$ km/s, $V_{S0,2} = 1.8$ km/s, $\rho_2 = 2.2$ gm/cm³, $\epsilon_2 = 0.3$, $\delta_2 = 0.15$, $\gamma_2 = 0.11$, $\nu_2 = 30^\circ$, and $\phi_2 = 30^\circ$.

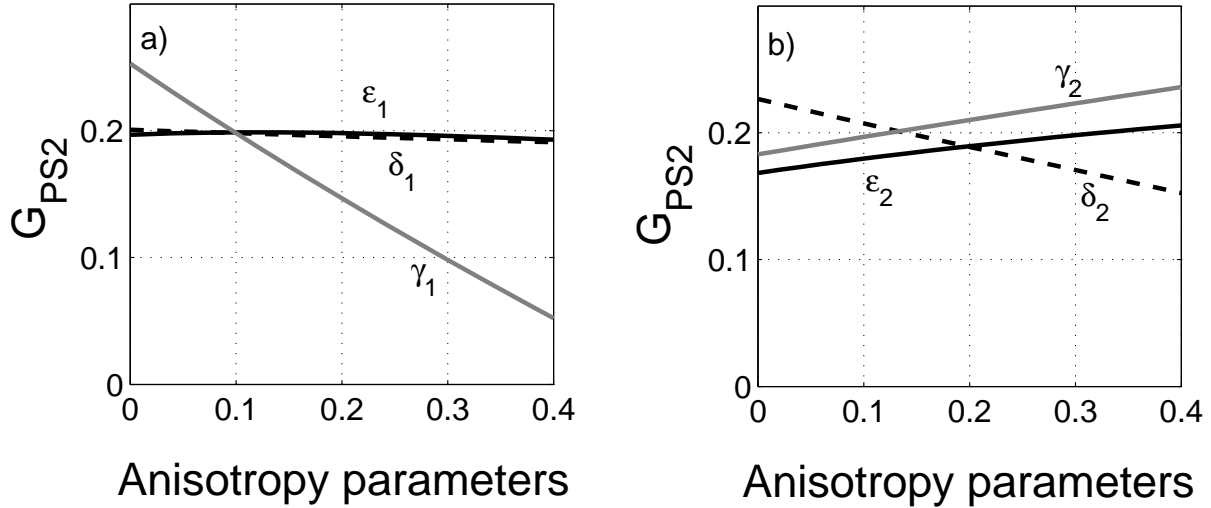


Figure 10. Exact AVO gradient of the PS_2 -wave for a TTI/TTI interface as a function of the anisotropy parameters in the (a) incidence and (b) reflecting halfspaces. The model is the same as in Figure 9.

4 DISCUSSION AND CONCLUSIONS

In the absence of lateral heterogeneity, anisotropy is the most likely reason for significant PS-wave energy at zero and small offsets observed in many multicomponent data sets. Here, we analyze the small-angle PS-wave AVO response for the most common type of anisotropy: transverse isotropy with a tilted symmetry axis (TTI medium). If the reflector does not coincide with a symmetry plane in either halfspace, a P-wave at normal

incidence always generates reflected PS-waves. To examine the influence of the anisotropy parameters on the normal-incidence PS-wave reflection coefficient and AVO gradient, we employ linearized analytic solutions (obtained using weak-contrast, weak-anisotropy approximations) supported by numerical modeling of the exact reflection coefficient.

If the incidence halfspace is isotropic, the reflected PS-wave is polarized in the symmetry-axis plane of the

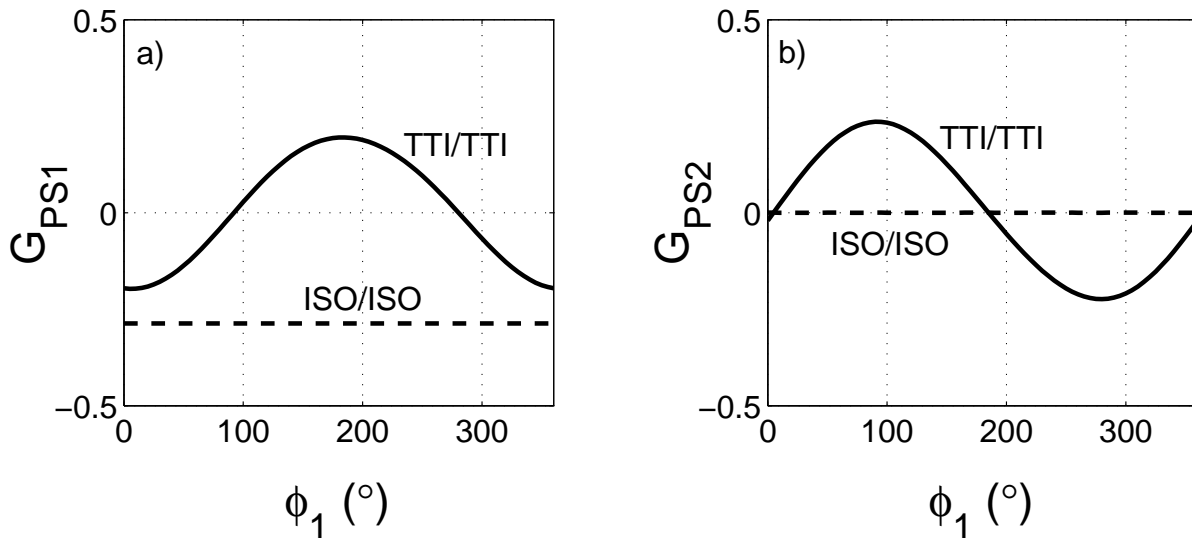


Figure 11. Exact AVO gradients of the (a) PS_1 - and (b) PS_2 -waves as functions of the azimuth ϕ_1 for a TTI/TTI interface (black solid line) and isotropic/isotropic interface (black dashed line). The parameters of the isotropic model are $V_{P,1} = 2.9$ km/s, $V_{S,1} = 1.5$ km/s, $\rho_1 = 2$ gm/cm³, $V_{P,2} = 3.3$ km/s, $V_{S,2} = 1.8$ km/s, and $\rho_2 = 2.2$ gm/cm³. For the TTI/TTI interface, the parameters are $V_{P0,1} = 2.9$ km/s, $V_{S0,1} = 1.5$ km/s, $\rho_1 = 2$ gm/cm³, $\epsilon_1 = 0.2$, $\delta_1 = 0.1$, $\gamma_1 = 0.1$, $\nu_1 = 60^\circ$, $V_{P0,2} = 3.3$ km/s, $V_{S0,2} = 1.8$ km/s, $\rho_2 = 2.2$ gm/cm³, $\epsilon_2 = 0.3$, $\delta_2 = 0.15$, $\gamma_2 = 0.11$, $\nu_2 = 30^\circ$, and $\phi_2 = 30^\circ$.

reflecting TTI medium. The normal-incidence reflection coefficient $R_{PS}(0)$ vanishes when the reflecting TI half-space is VTI or HTI, because in that case the model as a whole has a horizontal symmetry plane. The coefficient $R_{PS}(0)$ rapidly increases as the symmetry axis deviates from both the vertical and horizontal directions. Closed-form approximations and numerical modeling show that $R_{PS}(0)$ can reach values close to 0.1 for moderate values of the anisotropy parameters typical for shale formations. When the tilt ν_2 of the symmetry axis is relatively small, the coefficient $R_{PS}(0)$ is mostly controlled by δ_2 , with the contribution of ϵ_2 becoming dominant for larger values of ν_2 .

When both halfspaces are anisotropic (TTI), a P-wave at normal incidence excited two split PS-waves (PS_1 and PS_2) with the polarizations governed by the orientation of the symmetry axis in the incidence medium. The reflection coefficients of both PS-waves are functions of the difference between the azimuths of the symmetry axes ($\phi_2 - \phi_1$) and do not depend on either azimuth individually. The linearized normal-incidence reflection coefficient goes to zero when the two halfspaces have the same orientation of the symmetry axis and the same parameters ϵ and δ , even though there may be a jump in the velocities and densities across the interface.

We also discussed the azimuthally varying AVO gradients of PS-waves responsible for the small-angle reflection response. If the symmetry axis of the incidence halfspace is confined to the vertical incidence plane (or if the incidence halfspace is isotropic), the AVO

gradient of the PS_1 (PSV)-wave includes both purely isotropic and anisotropic terms, while the PS_2 (PSH)-wave AVO gradient is entirely anisotropic. For an arbitrary symmetry-axis orientation, however, neither AVO gradient contains purely isotropic terms since the contributions of the velocity and density contrasts are multiplied with functions of the symmetry-axis azimuth ϕ_1 . The AVO gradients are mostly influenced by the anisotropy in the incidence medium that causes shear-wave splitting and pronounced azimuthal variation of the reflection coefficients of both PS-waves.

The linearized approximations developed here not only provide physical insight into the behavior of the PS-wave reflection coefficients, but can be also used to quickly evaluate the PS-wave amplitudes for a wide range of TTI models. Potentially, these analytic expressions can help in the AVO inversion of PP and PS data for TTI media that can be implemented using the approach suggested by Jílek (2001) for anisotropic models with a horizontal symmetry plane.

5 ACKNOWLEDGMENTS

We are grateful to members of the A(nisotropy)-Team of the Center for Wave Phenomena (CWP), Colorado School of Mines and P. Jílek (BP Americas) for helpful discussions. The support for this work was provided by the Consortium Project on Seismic Inverse Methods for Complex Structures at CWP and by the Chemical Sci-

ences, Geosciences and Biosciences Division, Office of Basic Energy Sciences, U.S. Department of Energy.

REFERENCES

- Aki, K., and Richards, P. G. 1980, *Quantitative Seismology: Theory and methods: Vol.1.* W. N. Freeman & Co., San Francisco.
- Alvarez, K., Donati, M., and Aldana, M. 1999, AVO analysis for converted waves: 69th Annual Internat. Mtg., Soc. Expl. Geophys., Expanded Abstracts, 876-879.
- Artola, F. V. A., Leiderman, R., Fontoura, S. A. B., and Silva, M. B. C. 2003, Zero-offset C-wave reflectivity in horizontally layered media: 73rd Annual Internat. Mtg., Soc. Expl. Geophys., Expanded Abstracts, 761-764.
- Banik, N. C. 1987, An effective anisotropy parameter in transversely isotropic media: *Geophysics*, **52**, 1654-1664.
- Donati, S. M. 1998, Making AVO analysis for converted waves a practical issue: 68th Annual Internat. Mtg., Soc. Expl. Geophys., Expanded Abstracts, 2060-2063.
- Jech, J., and Pšenčík, I. 1989, First-order perturbation method for anisotropic media: *Geophys. J. Int.*, **99**, 369-376.
- Jílek, P. 2000, Converted PS-wave reflection coefficients in anisotropic media: CWP Annual Project Review, CWP-340, 275-299.
- , 2001, Modeling and inversion of converted-wave reflection coefficients in anisotropic media: A tool for quantitative AVO analysis: Ph.D. Thesis, Center for Wave Phenomena, Colorado School of Mines, Golden, Colorado.
- Larsen, A. J., Margrave, F. G., and Lu, H-X. 1999, AVO analysis by simultaneous P-P and P-S weighted stacking applied to 3C-3D seismic data: 69th Annual Internat. Mtg., Soc. Expl. Geophys., Expanded Abstracts, 721-724.
- Nefedkina, T., and Buzlukov, V. 1999, Seismic dynamic inversion using multiwave AVO data: 69th Annual Internat. Mtg., Soc. Expl. Geophys., Expanded Abstracts, 888-891.
- Pšenčík, I., and Vavryčuk, V. 1998, Weak contrast PP wave displacement R/T coefficients in weakly anisotropic elastic media: *Pure Appl. Geophys.*, **151**, 699-718.
- Rüger, A. 1996, Reflection coefficients and azimuthal AVO analysis in anisotropic media: Ph.D. Thesis, Center for Wave Phenomena, Colorado School of Mines, Golden, Colorado.
- , 1997, P-wave reflection coefficients for transversely isotropic models with vertical and horizontal axis of symmetry: *Geophysics*, **62**, 713-722.
- , 1998, Variation of P-wave reflectivity with offset and azimuth in anisotropic media: *Geophysics*, **63**, 935-947.
- Shuey, R. T. 1985, A simplification of Zoeppritz-equations: *Geophysics*, **50**, 609-614.
- Thomsen, L. 1993, Weak anisotropic reflections: In: *Offset dependent reflectivity* (Castagna and Backus, Eds.), SEG, Tulsa.
- , 2002, Understanding seismic anisotropy in exploration and exploitation: Distinguished Instructor Short Course (DISC), No. 5, SEG and EAGE.
- Tsvankin, I. 1995, *Seismic wavefields in layered isotropic media*: Samizdat Press, Colorado School of Mines.
- , 2001, *Seismic signatures and analysis of reflection data in anisotropic media*: Elsevier Science.
- Vavryčuk, V. 1999, Weak-contrast reflection/transmission coefficients in weakly anisotropic elastic media: P-wave incidence: *Geophys. J. Int.*, **138**, 553-562.
- Vavryčuk, V., and Pšenčík, I. 1998, PP-wave reflection coefficients in weakly anisotropic elastic media: *Geophysics*, **63**, 2129-2141.

APPENDIX A: PERTURBATION APPROACH APPLIED TO THE REFLECTION/TRANSMISSION PROBLEM

The approximate linearized reflection and transmission coefficients are derived by using an isotropic full space as the reference medium. A horizontal planar interface (reflector) divides the full space into two halfspaces, which are perturbed to obtain two weakly anisotropic media:

$$a_{ijkl}^{(I)} = a_{ijkl}^0 + \delta a_{ijkl}^{(I)}, \quad (\text{A1})$$

$$\rho^{(I)} = \rho^0 + \delta \rho^{(I)}, \quad (\text{A2})$$

$$|\delta a_{ijkl}^{(I)}| \ll \|a_{ijkl}^0\|, \quad (\text{A3})$$

$$|\delta \rho^{(I)}| \ll \rho^0. \quad (\text{A4})$$

In equation (A4), the index I ($I = 1, 2$) stands for the incidence and reflecting halfspaces, respectively, and $a_{ijkl}^{(I)}$ and ρ^0 are the density-normalized stiffness coefficients and density of the background isotropic medium. Since the perturbations from the isotropic background in both halfspaces are small, the approximation involves both weak anisotropy and weak elastic contrast between the halfspaces. Using these approximations, the polarization ($\mathbf{p}^{(N)}$) and slowness vectors ($\mathbf{g}^{(N)}$) can be linearized as follows:

$$\begin{aligned} \mathbf{g}^{(N)} &\approx \mathbf{g}^{0(N)} + \delta \mathbf{g}^{(N)}, \\ \mathbf{p}^{(N)} &\approx \mathbf{p}^{0(N)} + \delta \mathbf{p}^{(N)}, \end{aligned} \quad (\text{A5})$$

where $\mathbf{g}^{0(N)}$ and $\mathbf{p}^{0(N)}$ are the polarization and slowness vectors of waves propagating in the background isotropic medium, and $\delta \mathbf{g}^{(N)}$ and $\delta \mathbf{p}^{(N)}$ are their linear perturbations. Analytic expressions for the perturbations $\delta \mathbf{g}^{(N)}$ and $\delta \mathbf{p}^{(N)}$ in terms of $\delta a_{ijkl}^{(I)}$ are given in Vavryčuk and Pšenčík (1998) and Jílek (2000). Substituting these linearized expressions into equation (1) of the main text yields

$$(\mathbf{C}^0 + \delta \mathbf{C})(\mathbf{U}^0 + \delta \mathbf{U}) = \mathbf{B}^0 + \delta \mathbf{B}. \quad (\text{A6})$$

Here, \mathbf{C}^0 is the stiffness matrix of the background medium and $\delta \mathbf{U}$ is the perturbation of the reflection and transmission coefficients in the background isotropic medium (\mathbf{U}^0). As the background is homogeneous, \mathbf{U}^0 is given by

$$\mathbf{U}^0 = [0, 0, 0, 0, 0, 1]^T. \quad (\text{A7})$$

Expanding equation (A6) and retaining only the leading terms in small quantities results in the following equation:

$$\delta \mathbf{U} = (\mathbf{C}^0)^{-1}(\delta \mathbf{B} - \delta \mathbf{C} \cdot \mathbf{U}^0), \quad (\text{A8})$$

where

$$\delta \mathbf{C} = \begin{bmatrix} \delta g_1^{(1)} & \delta g_1^{(2)} & \delta g_1^{(3)} & -\delta g_1^{(4)} & -\delta g_1^{(5)} & -\delta g_1^{(6)} \\ \delta g_2^{(1)} & \delta g_2^{(2)} & \delta g_2^{(3)} & -\delta g_2^{(4)} & -\delta g_2^{(5)} & -\delta g_2^{(6)} \\ \delta g_3^{(1)} & \delta g_3^{(2)} & \delta g_3^{(3)} & -\delta g_3^{(4)} & -\delta g_3^{(5)} & -\delta g_3^{(6)} \\ \delta X_1^{(1)} & \delta X_1^{(2)} & \delta X_1^{(3)} & -\delta X_1^{(4)} & -\delta X_1^{(5)} & -\delta X_1^{(6)} \\ \delta X_2^{(1)} & \delta X_2^{(2)} & \delta X_2^{(3)} & -\delta X_2^{(4)} & -\delta X_2^{(5)} & -\delta X_2^{(6)} \\ \delta X_3^{(1)} & \delta X_3^{(2)} & \delta X_3^{(3)} & -\delta X_3^{(4)} & -\delta X_3^{(5)} & -\delta X_3^{(6)} \end{bmatrix}, \quad (\text{A9})$$

$$\delta \mathbf{B} = - \left[\delta g_1^{(0)}, \delta g_2^{(0)}, \delta g_3^{(0)}, \delta X_1^{(0)}, \delta X_2^{(0)}, \delta X_3^{(0)} \right]^T. \quad (\text{A10})$$

Therefore, the perturbed vector of the reflection/transmission coefficients is obtained as

$$\delta \mathbf{U} = (\mathbf{C}^0)^{-1} \begin{bmatrix} \delta g_1^{(6)} - \delta g_1^{(0)}, & \delta g_2^{(6)} - \delta g_2^{(0)}, & \delta g_3^{(6)} - \delta g_3^{(0)}, \\ \delta X_1^{(6)} - \delta X_1^{(0)}, & \delta X_2^{(6)} - \delta X_2^{(0)}, & \delta X_3^{(6)} - \delta X_3^{(0)} \end{bmatrix}. \quad (\text{A11})$$

APPENDIX B: APPROXIMATE PS-WAVE AVO GRADIENTS IN TI MEDIA

Here, we present linearized expressions for the PS₁- and PS₂-wave AVO gradients (G_{PS_1} and G_{PS_2}) obtained in the weak-contrast, weak-anisotropy limit. If the incidence halfspace is isotropic, PS₁ becomes the PSV-wave with an

in-plane polarization, and PS₂ becomes the transversely polarized PSH-wave.

$$\begin{aligned}
 G_{PSV} = G_{PS_1} &= -\frac{2\Delta\beta}{g\beta} - \frac{(2+g)\Delta\rho}{2g\bar{\rho}} - \frac{2\sin^2\nu_2\sin^2\phi_2\gamma_2}{g} \\
 &+ \frac{g}{16(1+g)} \{ (3+2g)\delta_2 + (3-2g)\cos 4\nu_2(\delta_2 - \epsilon_2) - (1+2g)\epsilon_2 \\
 &\quad + 2\cos 2\nu_2[\delta_2 + 2(-1+2g)\cos 2\phi_2\sin^2\nu_2(\delta_2 - \epsilon_2) + 2\epsilon_2] \\
 &\quad + 4\cos 2\phi_2\sin^2\nu_2(2g\delta_2 - \epsilon_2 - 2g\epsilon_2) \}, \tag{B1}
 \end{aligned}$$

$$\begin{aligned}
 G_{PSH} = G_{PS_2} &= \frac{\sin^2\nu_2\sin 2\phi_2\gamma_2}{g} \\
 &+ \frac{g\sin^2\nu_2\sin 2\phi_2}{4(1+g)} \{ [2g + (-1+2g)\cos 2\nu_2](\delta_2 - \epsilon_2) - \epsilon_2 \}. \tag{B2}
 \end{aligned}$$

The AVO gradients for a TTI/TTI interface are given here only for the incidence plane containing the symmetry axis of the incidence TTI halfspace ($\phi_1 = 0^\circ$):

$$\begin{aligned}
 G_{PS_1} &= -\frac{2\Delta\beta}{g\beta} - \frac{(2+g)\Delta\rho}{2g\bar{\rho}} - \frac{2\sin^2\nu_2\sin^2\phi_2\gamma_2}{g} \\
 &+ \frac{g}{16(1+g)} \{ -4(1+g)(\delta_1 - \epsilon_1) + 4(-1+g)\cos 4\nu_1(\delta_1 - \epsilon_1) \\
 &\quad - 8\cos 2\nu_1\epsilon_1 + 3\delta_2 - \epsilon_2 + 2g(\delta_2 - \epsilon_2) + 2\cos 2\nu_2(\delta_2 + 2\epsilon_2) \\
 &\quad + 4\cos 2\phi_2\sin^2\nu_2\{-\epsilon_2 + [2g + (-1+2g)\cos 2\nu_2](\delta_2 - \epsilon_2)\} \\
 &\quad + (3-2g)\cos 4\nu_2(\delta_2 - \epsilon_2) \}, \tag{B3}
 \end{aligned}$$

$$\begin{aligned}
 G_{PS_2} &= \frac{\sin^2\nu_2\sin 2\phi_2\gamma_2}{g} \\
 &+ \frac{g\sin^2\nu_2\sin 2\phi_2}{4(1+g)} \{ [2g + (-1+2g)\cos 2\nu_2](\delta_2 - \epsilon_2) - \epsilon_2 \}. \tag{B4}
 \end{aligned}$$

If the symmetry axis of the upper halfspace deviates from the incidence plane, fully linearized AVO gradients can still be derived for the special case of the incidence HTI medium:

$$\begin{aligned}
 G_{PS_1} &= -\frac{2\Delta\beta\cos\phi_1}{g\beta} - \frac{(2+g)\Delta\rho\cos\phi_1}{2g\bar{\rho}} - \frac{2\sin^2\nu_2\sin(\phi_2 - \phi_1)\sin\phi_2\gamma_2}{g} \\
 &+ \frac{g}{16(1+g)} \{ 4\sin^2\nu_2\cos(2\phi_2 - \phi_1) \{ [2g + (-1+2g)\cos 2\nu_2](\delta_2 - \epsilon_2) - \epsilon_2 \} \\
 &\quad + \cos\phi_1[-8\delta_1 + 16\epsilon_1 + 3\delta_2 - \epsilon_2 + 2g(\delta_2 - \epsilon_2) \\
 &\quad + 2\cos 2\nu_2(\delta_2 + 2\epsilon_2) - (-3+2g)\cos 4\nu_2(\delta_2 - \epsilon_2)] \}, \tag{B5}
 \end{aligned}$$

$$\begin{aligned}
 G_{PS_2} &= \frac{2\Delta\beta\sin\phi_1}{g\beta} + \frac{(2+g)\Delta\rho\sin\phi_1}{2g\bar{\rho}} - \frac{2\sin\phi_1\gamma_1}{g} \\
 &+ \frac{2\sin^2\nu_2\cos(\phi_2 - \phi_1)\sin\phi_2\gamma_2}{g} \\
 &+ \frac{g}{16(1+g)} \{ 4\sin^2\nu_2\sin(2\phi_2 - \phi_1) \{ [2g + (-1+2g)\cos 2\nu_2](\delta_2 - \epsilon_2) - \epsilon_2 \} \\
 &\quad - \sin\phi_1[3\delta_2 - \epsilon_2 + 2g(\delta_2 - \epsilon_2) + 2\cos 2\nu_2(\delta_2 + 2\epsilon_2) \\
 &\quad - (-3+2g)\cos 4\nu_2(\delta_2 - \epsilon_2)] \}. \tag{B6}
 \end{aligned}$$

